Human Molecular Genetics, 2012, Vol. 21, No. 11 **2559–2571**
doi:10.1093/hmg/dds082
Advance Access published on March 2, 2012

Rescue of severely affected dystrophin/utrophin-deficient mice through scAAV-U7snRNA-mediated exon skipping

Aurélie Goyenvalle[1,2,*], Arran Babbs[1], Jordan Wright[1], Vivienne Wilkins[1], Dave Powell[1], Luis Garcia[2] and Kay E. Davies[1,*]

[1]MRC Functional Genomics Unit, Department of Physiology, Anatomy and Genetics, University of Oxford, Oxford, UK and [2]Biothérapies des Maladies Neuromusculaires Unité Mixte: Um76 UPMC, UMR 7215 CNRS, U974, Inserm, Institut de Myologie, Faculté de Médecine Pierre et Marie Curie, Paris, France

Received November 16, 2011; Revised February 6, 2012; Accepted February 24, 2012

Duchenne muscular dystrophy (DMD) is a severe neuromuscular disorder caused by mutations in the dystrophin gene that result in the absence of functional protein. Antisense-mediated exon skipping is one of the most promising approaches for the treatment of DMD and recent clinical trials have demonstrated encouraging results. However, antisense oligonucleotide-mediated exon skipping for DMD still faces major hurdles such as extremely low efficacy in the cardiac muscle, poor cellular uptake and relatively rapid clearance from circulation, which means that repeated administrations are required to achieve some therapeutic efficacy. To overcome these limitations, we previously proposed the use of small nuclear RNAs (snRNAs), especially U7snRNA to shuttle the antisense sequences after vectorization into adeno-associated virus (AAV) vectors. In this study, we report for the first time the efficiency of the AAV-mediated exon skipping approach in the utrophin/dystrophin double-knockout (dKO) mouse which is a very severe and progressive mouse model of DMD. Following a single intravenous injection of scAAV9-U7ex23 in dKO mice, near-normal levels of dystrophin expression were restored in all muscles examined, including the heart. This resulted in a considerable improvement of their muscle function and dystrophic pathology as well as a remarkable extension of the dKO mice lifespan. These findings suggest great potential for AAV-U7 in systemic treatment of the DMD phenotype.

INTRODUCTION

Duchenne muscular dystrophy (DMD) is a severe muscle-wasting disorder affecting 1:3500 live male births, caused by mutations in the dystrophin gene. The majority of mutations disrupt the open reading frame, resulting in the absence of a functional dystrophin protein at the sarcolemma of muscle fibres. The related allelic disorder Becker muscular dystrophy (BMD) is caused by mutations that create shortened but in-frame transcripts with production of partially functional dystrophin, leading to a milder phenotype (1). One of the most promising therapeutic strategy for DMD aims to convert an out-of-frame mutation into an in-frame mutation, which would give rise to internally deleted, but still functional dystrophin (1,2). This can be achieved using antisense oligonucleotides (AOs) that interfere with splice sites or regulatory elements within the exon and thus induce the skipping of specific exons at the pre-mRNA level (3,4). The applicability of AO therapy has now been demonstrated in Phase I/II clinical trials with two different chemistries of AOs targeting the human dystrophin exon 51 in DMD patients (5,6). More recently, the systemic treatment of DMD patients with AOs was reported to induce dose-dependent exon-skipping efficacy leading to detectable amounts of dystrophin protein in skeletal muscles of patients treated with 2 mg or more per kilogram (7,8). These preliminary results appear promising and raise expectations to a high level for

*To whom correspondence should be addressed at: MRC Functional Genomics Unit, Department of Physiology, Anatomy and Genetics, University of Oxford, South Parks Road, OX1 3PT Oxford, UK. Tel: +44 1865285880; Fax: +33 153600802; E-mail: aurelie.goyenvalle@dpag.ox.ac.uk (A.G.); Fax: +44 1865285878; E-mail: kay.davies@dpag.ox.ac.uk (K.E.D.).

the systemic treatment of DMD. However, many hurdles remain, especially regarding the personalized medicine nature of the strategy and the challenging delivery to all affected tissues in DMD (9). Both chemistries used in clinical trials, 2′-*O*-methyl phosphorothioate (2OMePS) and phosphorodiamidate morpholino oligomers (PMO), are still limited by the poor cellular uptake and relatively rapid clearance from circulation, which means that repeated administrations are necessary to achieve some therapeutic efficacy. One way of circumventing this is to deliver the antisense sequence using viral vectors. We and others have previously demonstrated that small nuclear RNA (snRNA) such as U1 and U7snRNA could induce efficient exon-skipping *in vitro* and *in vivo* when appropriately modified with specific antisense sequences (10,11). The antisense sequence embedded into an snRNP particle is protected from degradation and accumulates in the nucleus where splicing occurs. When introduced into adeno-associated virus (AAV) vectors, these snRNAs can induce long-term restoration of dystrophin which represents a strong advantage of this approach over synthetic AOs by eliminating the need for repeated injections.

A second hurdle with the systemic administration of AOs is the high variability in exon-skipping efficiency among muscle types. Data collected from mouse and dog studies have shown that some muscles respond better than others (12–14). Even within the most responsive muscles, dystrophin was not uniformly expressed, with patches of both dystrophin-positive fibres and dystrophin-negative fibres observed. Moreover, both 2OMePS and PMO AOs have shown very little efficacy in the heart (12,15), which is currently a major challenge to the therapeutic potential of AOs. AAV vectors on the other hand are a powerful tool to deliver therapeutic genes to the skeletal muscle (16) and several serotypes of AAV show specific tropisms to skeletal and cardiac muscles (17,18). The AAV serotype 9 in particular has been reported to transduce the heart very efficiently (18), as well as most of the skeletal muscles.

In this study, we investigated the therapeutic potential of systemic AAV9-mediated exon skipping in a severely affected mouse model of DMD. While the dystrophin-deficient *mdx* mouse has historically been used as the primary model of DMD, the dystrophin/utrophin double-knockout (dKO) mouse suffers from a much more severe and progressive muscle wasting, impaired mobility and premature death (19,20).

We therefore tested the hypothesis that the AAV-U7snRNA-mediated exon skipping we previously used in *mdx* mice (11) could ameliorate the pathology associated with severe muscular dystrophy in dKO mice. We demonstrate that a single injection of self-complementary AAV9 vector (scAAV9) encoding a modified U7snRNA specific to exon 23 of the dystrophin pre-mRNA induces a widespread restoration of dystrophin expression in all muscles examined, including the heart. This leads to a considerable improvement of the dystrophic phenotype of these mice and a remarkable extension of lifespan.

RESULTS

Widespread dystrophin expression in dKO mice after scAAV9-U7ex23 injection

Self-complementary AAV vectors (scAAV) have been reported to induce higher transduction efficiencies than conventional single-stranded AAV vectors (ssAAV) by circumventing the need to convert the single-stranded DNA genome into double-stranded DNA prior to expression (21). We therefore decided to use this type of vector for our systemic study in the dKO mouse model. The modified U7snRNA specific to exon 23 of the dystrophin pre-mRNA (U7ex23) (11) was inserted between the inverted terminal repeats (ITRs) of a plasmid self complementary adenoviral associated vector (pscAAV) construct, and scAAV pseudotyped with a serotype 9 capsid were subsequently produced for optimum skeletal and cardiac muscle delivery. dKO mice received a single intravenous (i.v.) injection of $\sim$1E + 13 vg of scAAV9-U7ex23 at 3 weeks of age. Control dKO mice display a severe dystrophic phenotype from an early age (sometimes as early as 5 weeks of age) and were sacrificed at a humane endpoint which varied between 6 and 18 weeks of age depending on the severity of their pathology (average lifespan of 10.2 weeks). While some scAAV9-treated dKO mice were kept for long-term analysis, six were sacrificed at 12 weeks of age (9 weeks after injection) for muscle analysis.

Total RNA extracted from the treated muscles was analysed by reverse transcriptase–polymerase chain reaction (RT–PCR) (Fig. 1A). The full-length transcript is represented by an amplicon of 901 bp, and the in-frame transcript excluding the mutated exon 23 is represented by a 688 bp product. The scAAV9 injection induced a very efficient exon 23 skipping in all skeletal muscles examined, where the skipped product was the major product detected (Fig. 1A). Skipping efficiency appeared particularly high in the heart where the full-length transcript was hardly detectable. The shorter 542 bp amplicon corresponds to a skipped transcript lacking exons 22 and 23 and has been reported previously (4,22).

In order to quantify more accurately the levels of exon skipping in each muscle group, quantitative PCR was performed using Taqman assays that were designed against the dystrophin exon 4–5 or exon 22–24 templates using the Custom Assay Design Tool (Applied Biosystems). The percentage of exon 23 skipping was expressed as a percentage of total dystrophin as indicated by the exon 4–5 expression level, after normalization with an endogenous control. Exon 23 skipping levels ranged from $\sim$20% in the diaphragm to 50% in the heart (Fig. 1B). Despite being generally lower, the levels of exon skipping measured by quantitative PCR (qPCR) correlated with the nested RT–PCR results. This discrepancy was somewhat expected as it has previously been demonstrated that nested RT–PCR may lead to overestimation of exon-skipping levels (23).

Western blotting was performed on samples from treated dKO mice to evaluate the restoration of dystrophin protein. Results presented in Figure 1C and D confirmed the RT–PCR data as dystrophin expression was detected in all muscles examined. Quantification of the observed bands revealed levels of dystrophin restoration between 45 and 95% of wild-type levels (Fig. 1D). Of particular significance was the cardiac muscle, where dystrophin rescue was almost complete, reflecting the favourable tropism of the AAV serotype 9 for the heart.

Immunofluorescence performed on tissue sections confirmed restoration of dystrophin and its correct localization at the membrane of the sarcolemma in all muscles analysed

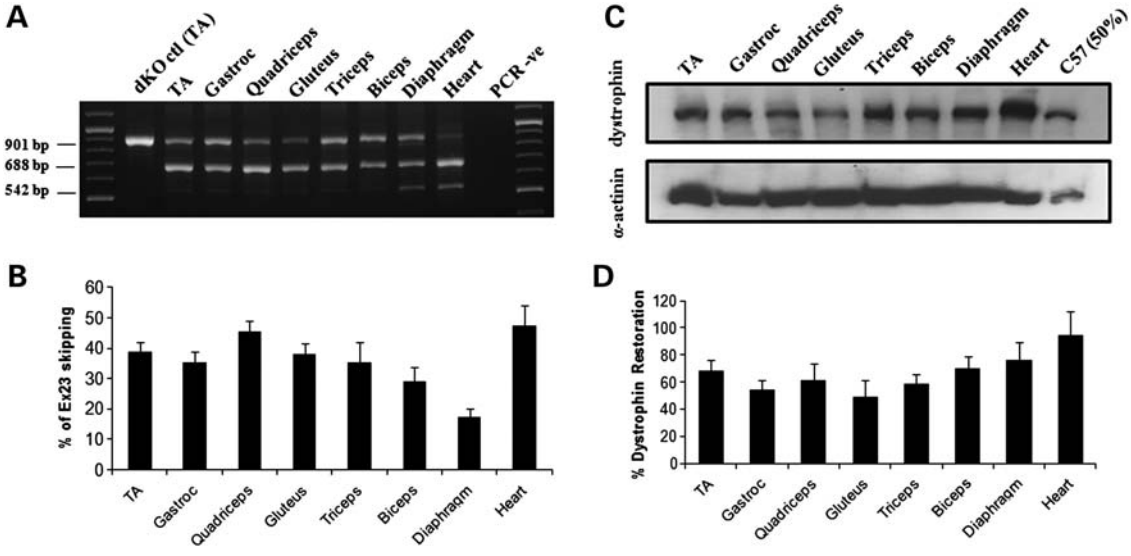

Figure 1. Exon-skipping and dystrophin expression in tissues from dKO mice following one i.v. injection of scAAV9-U7ex23. (**A**) RT–PCR analysis to detect exon 23 skipping efficiency at the RNA level. The 901 bp product represents the full-length transcript, and the products of 688 and 542 bp represent transcripts that exclude exon 23 and exons 22 and 23, respectively. (**B**) Quantification of exon 23 skipping measured by Taqman qPCR. Exon 23 skipping is expressed as a percentage of total dystrophin, measured by the exon 4–5 expression level, after normalization with an endogenous control ($n = 6$). (**C**) Western blot to detect dystrophin expression in tissues from scAAV9-treated dKO mice, compared with C57BL6 control mice (top gel). Equal loading of 100 μg protein is shown for each sample with α-actinin expression detected as a loading control except for the C57BL6 samples for which only 50 μg was loaded (bottom gel). (**D**) Quantification of levels of dystrophin protein restored in various muscles. Membranes were converted to numerical pictures by scanning, and band intensities were analysed using the ImageJ 1.33a software. Dystrophin levels are expressed as percentage compared with levels in wild-type tissue.

(Fig. 2). Widespread expression of dystrophin protein over multiple sections within each muscle group was detected in the forelimb (biceps and triceps), hind limb [tibialis anterior (TA)—as illustrated in Supplementary Material, Fig. S1, gastroc and quadriceps] and diaphragm muscles. As predicted by RT–PCR and western blot results, the level of dystrophin expression was particularly high in the cardiac muscle which was almost undistinguishable from the normal C57BL6 heart.

A small group of dKO mice were also injected with a limited dose of scAAV9-U7ex23 (between 1 and 2 E + 12 vg), which induced only low levels of exon 23 skipping and dystrophin restoration (Supplementary Material, Fig. S2). These levels of dystrophin expression (~10–15% in most muscles, except in the heart where levels are high) were not sufficient to significantly improve the dKO phenotype, suggesting a threshold of vector genomes necessary to restore adequate levels of dystrophin in the severe dKO model.

scAAV9-U7ex23 injection averts the onset of dystrophic pathology in the dKO mice

In order to evaluate the functional correction induced by exon-skipping, we first assessed the histopathology of the treated muscles. Histologically, dKO muscles are characterized by large inflammatory infiltrates and a high percentage of centrally nucleated myofibres, which reflect the continuous degeneration–regeneration process. Haematoxylin and eosin staining revealed a significant improvement of the muscle histopathology after exon-skipping treatment (Fig. 3A). sc-AAV9-treated muscles displayed noticeably fewer infiltrating mononuclear cells as well as a drastic reduction in the percentage of centrally nucleated myofibres (~28%) when compared with age-matched untreated dKO mice (~89%) (Fig. 3B). In addition, while dKO muscles showed an increased number of small fibres as a result of the degeneration–regeneration cycles, treated muscles revealed a uniformity of the muscle fibres similar to that observed in the C57BL6 controls, reflecting the functionality of the restored dystrophin (Fig. 3A).

Next, we evaluated the restoration of the dystrophin-associated protein complex (DAPC). Dystrophin and the DAPC play a major structural role in muscles by forming a link between the internal cytoskeleton actin and the extracellular matrix, but the DAPC also has important signalling functions via other components (24,25). In the absence of functional dystrophin protein, the DAPC fails to localize correctly at the sarcolemma and its function is therefore compromised. Staining of muscles sections from scAAV9-treated dKO mice revealed the expression of the DAPC component proteins including α-sarcoglycan, β-sarcoglycan and β-dystroglycan and, more importantly, their correct localization at the sarcolemma (Fig. 3C).

scAAV9-U7ex23 injection improves muscle function and remarkably extends lifespan of dKO mice

Encouraged by the widespread restoration of dystrophin expression and the improvement of the muscle histopathology following the scAAV9-U7ex23 injection, we investigated in more detail the function and contractile properties of the treated muscles. We first assessed the forelimb muscle strength of the treated and control mice using a functional test of grip force strength (26,27). As expected, untreated dKO mice displayed a reduced grip strength compared with

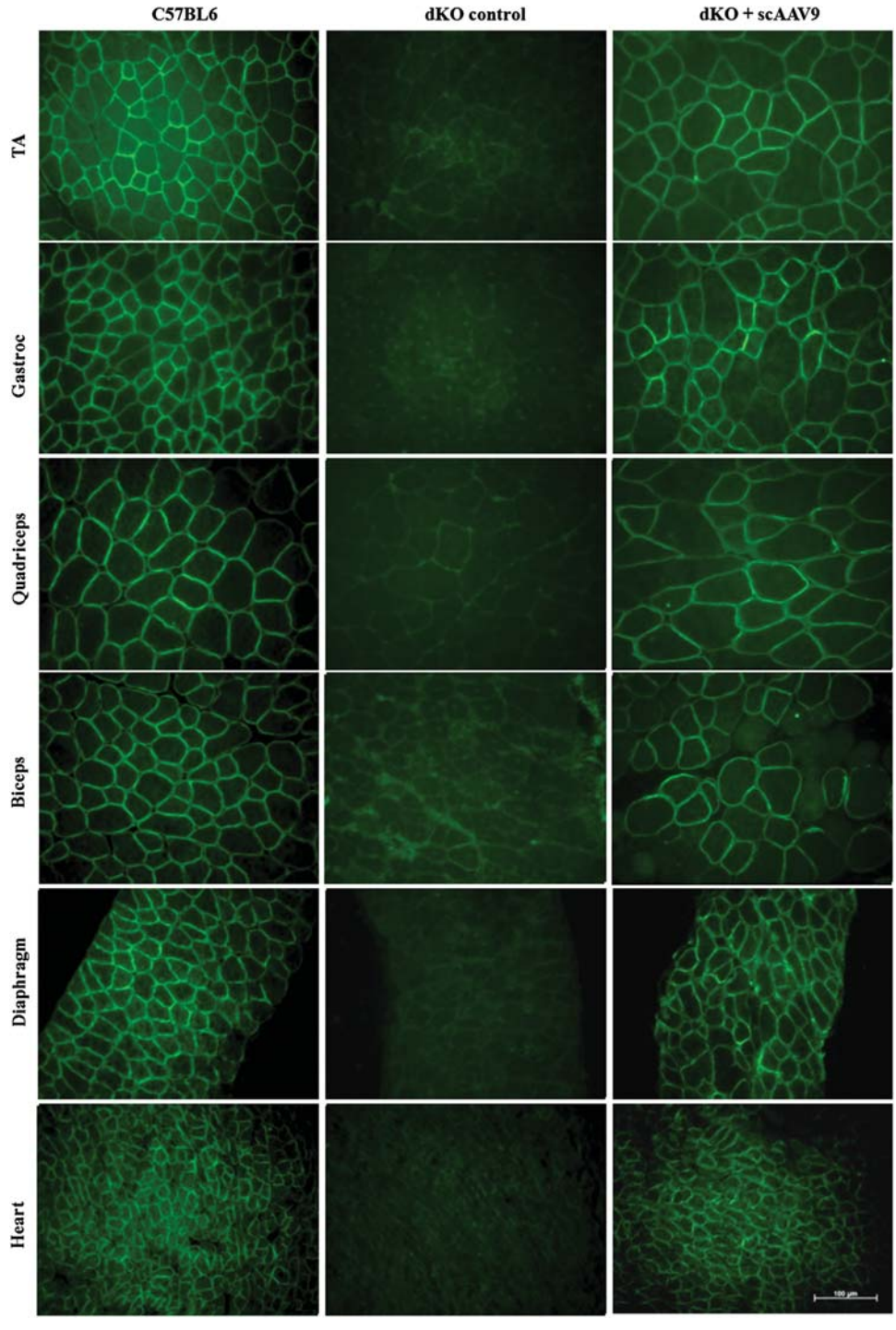

Figure 2. Dystrophin restoration in treated dKO muscles. Immunostaining of muscle tissue cross-sections to detect dystrophin expression and localization in C57BL6 normal control mice (left panel), untreated dKO mice (middle panel) and scAAV9-U7ex23-treated mice (right panel). Tissues analysed were from TA, gastrocnemius, quadriceps, biceps, diaphragm and heart muscles (scale bar = 100 μm).

age-matched C57BL6 controls as illustrated in Figure 4A. scAAV9-treated dKO on the other hand showed a significant improvement of their grip strength, comparable to that of the normal controls. We next investigated force production in hind limb muscles of treated and control mice using the extensor digitorum longus (EDL) muscle. As a result of the severe muscle degeneration in dKO mice, specific force appeared reduced in untreated dKO mice compared with C57BL6 controls (Fig. 4B). scAAV9-U7ex23 treatment considerably improved dKO muscle function such that specific force was no longer significantly different from that generated by wild-type mice (Fig. 4B).

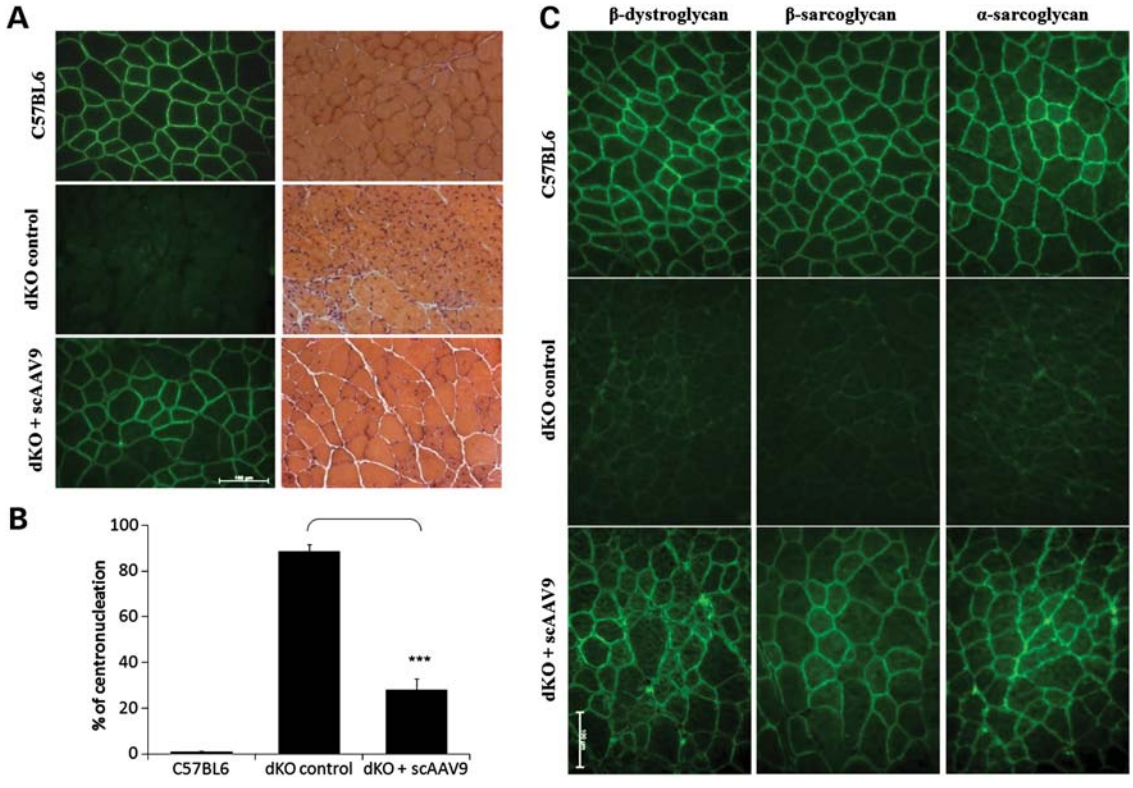

Figure 3. scAAV-U7ex23 treatment improves muscle histopathology in dKO mice. (**A**) The left panel shows immunofluorescent staining for dystrophin (green) of tibialis anterior cross-sections from C57BL6 normal control mice (up), untreated dKO mice (middle) and peptide conjugated PMO treated mice (bottom). The lower panel shows haematoxylin and eosin staining of the same muscles. (**B**) Percentage of myofibres with centronucleation ($n = 600–1800$ myofibres/cohort). $^{***}P < 0.001$ when compared with untreated dKO mice. (**C**) Expression of dystrophin restores the DAPC to the sarcolemma in the scAAV9-treated dKO mice. DAPC components α- and β-sarcoglycan and β-dystroglycan were detected by immunostaining in tissue cross-section of TA muscles from scAAV9-treated dKO mice (lower panel), compared with C57BL6 normal mice (upper panel) and untreated dKO mice (middle panel) (scale bar = 100 μm).

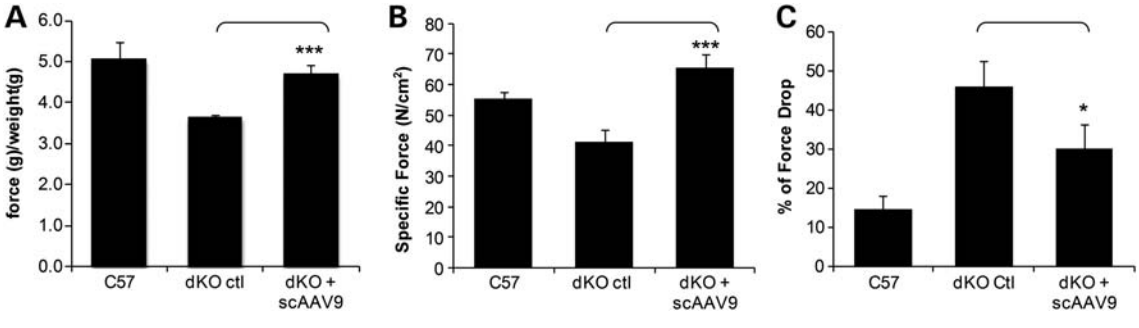

Figure 4. Improvement of muscle function in scAAV9-treated mice. (**A**) Forelimb muscle function assessment shows the physical improvement of scAAV-treated dKO mice compared with untreated dKO mice and C57BL6 normal control mice ($n = 6$ per cohort). $^{***}P < 0.005$ compared with untreated dKO mice. (**B**) EDL muscles of scAAV-treated dKO mice were analysed for their maximal force (peak force) producing capacity compared with untreated dKO mice and C57BL6 control mice. Maximal force was also normalized for cross-sectional area to assess specific force. $^{***}P < 0.005$ compared with untreated dKO mice. Specific force is not significantly different between treated dKO and C57Bl6 ($P > 0.09$). (**C**) The percentage of force drop is assessed by measuring the force deficit following a series of five eccentric contractions. $^{*}P < 0.05$ compared with untreated dKO mice. Error bars are shown as mean ± SEM ($n = 6$ per cohort).

In addition, we tested the ability of the restored dystrophin to protect dKO myofibres from exercise-induced damage, by assessing maintenance of force production following a series of eccentric contractions. The protocol applied resulted in a reduction in initial muscle contractile force of ∼46% in untreated dKO mice compared with only ∼14% in C57Bl6 mice (Fig. 4C). Treated dKO muscles appeared somewhat protected from contraction-induced injury as the percentage of force drop was reduced to ∼30%. Taken together, these results indicate that the widespread restoration of dystrophin expression induced by the scAAV9-U7ex23-mediated exon skipping greatly improves muscle function in the severely affected dKO mice.

In contrast to *mdx* mice, dKO mice display a very severe dystrophic phenotype, including abnormal waddling gait, contracted and stiff limbs, and very pronounced kyphosis as a

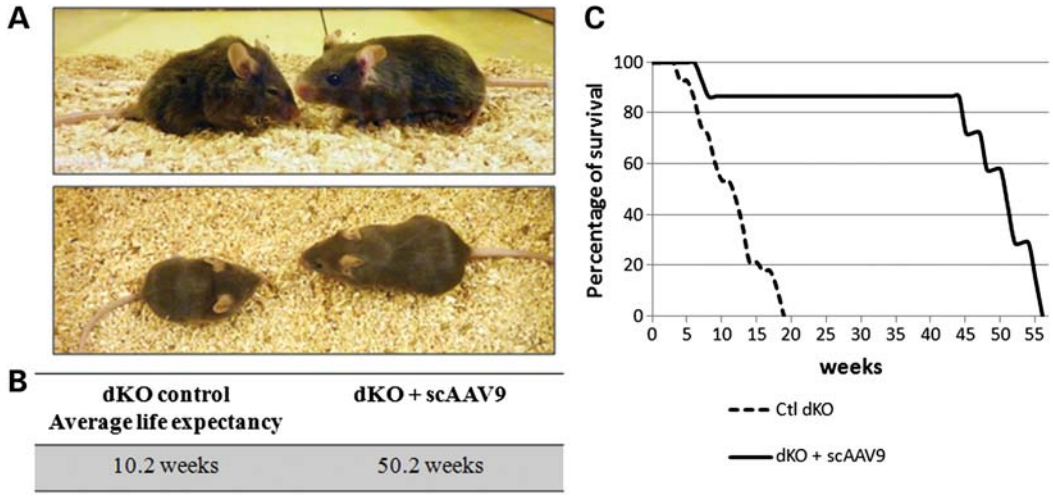

Figure 5. scAAV9-U7ex23 treatment averts the onset of dystrophic pathology in the dKO mice. (**A**) Photograph of an untreated dKO mouse at 12 weeks of age (left), displaying a strong kyphosis and joint contractures compared with an scAAV9-U7ex23-treated mouse at 24 weeks of age (right), looking healthy. (**B**) Average lifespan of untreated dKO and scAAV9-U7ex23-treated dKO mice. (**C**) Survival curves of untreated dKO (dash line) and scAAV9-U7ex23-treated dKO mice (continuous line).

result of the degenerative process (Fig. 5A). The reduced musculature considerably affects the mobility of the mice, especially during the last few weeks of life. Supplementary Material, Video S1, illustrates this seriously decreased ambulation in a 12-week-old control dKO mouse. This severe and progressive muscle wasting leads to premature death of the dKO mice between 6 and 18 weeks of age depending on the severity of their pathology (an average lifespan of 10.2 weeks; Fig. 5B and C).

The appearance and behaviour of scAAV9-treated dKO mice was strikingly different as demonstrated in Figure 5A and Supplementary Material, Video S2, in which the contrast between untreated control and treated dKO mice is clearly observable. The dystrophic pathology of treated mice appeared greatly improved as the animals demonstrated only a minimal kyphosis and contracted limbs (Fig. 5A). Furthermore, their mobility, their food-seeking behaviour and the turgor of the tail were markedly improved and appeared close to normal.

In order to measure more accurately the improvement of the dystrophic pathology in treated dKO mice, mice were monitored using open-field behavioural activity cages (28). scAAV9-U7ex23-treated dKO mice show significant improvement compared with age-matched untreated controls for most of the recorded parameters, 12 of which are shown in Figure 6A. Total activity, active time, rearing time and distance travelled, which are considered some of the best parameters for activity monitoring, are also represented as graphs in Figure 6B. Treated mice were shown to be significantly more active, travel further and rear more than the untreated controls, confirming the impressive improvement of their dystrophic pathology following a single injection of scAAV9-U7ex23.

While six scAAV9-treated dKO mice were sacrificed at 12 weeks of age for muscle analysis, six others were kept for long-term analysis to investigate the effect of exon skipping on lifespan. Remarkably, treated dKO mice still appeared healthy and active when older as illustrated in Supplementary Material, Video S3, of an 11-month-old-treated dKO mouse, reflecting the long-term effect of AAV vectors.

dKO mice treated with a single injection of scAAV9-U7ex23 at 3 weeks of age survived for ~1 year (an average lifespan of 50.2 weeks, $n = 6$), which represents a considerable improvement compared with untreated dKO mice (Fig. 5B and C). Analysis of muscles from treated dKO mice close to the endpoint revealed that exon 23 skipping and dystrophin expression were still detected nearly 1 year after the injection (Fig. 7), albeit levels being lower than those observed at 12 weeks of age. Levels of skipping and dystrophin appeared particularly lower in some hind limb muscles and the diaphragm, compared with the heart where dystrophin expression was still very high, which correlated with the detection of U7dtex23 transgene (Supplementary Material, Fig. S3).

Biomarkers levels dramatically improved after scAAV9-U7ex23 injection

Various biomarkers characteristic of muscular dystrophies, such as levels of creatine kinase in the serum have been identified over the years and have been used as valuable tools for the diagnosis of DMD. More recently, levels of specific muscle microRNAs (miRNAs), released into the bloodstream of DMD patients, have been described to correlate with the severity of the disease as a consequence of fibre damage (29). The same miRNAs have also been shown to be abundant in the blood of *mdx* mice and recover to wild-type levels in animals rescued through AO-mediated exon skipping (29). We therefore wanted to investigate the levels of these miRNAs in our scAAV-treated dKO mice compared with untreated dKO and healthy controls. Since these biomarkers can be analysed from the serum, they represent ideal tools to monitor the outcomes of therapeutic interventions, especially in our older scAAV9-treated dKO mice without the need to

A

Parameters measured by activity cage		dKO control	dKO + scAAV9	summary dKO vs dKO + scAAV9
Total activity	In beam breaks	271.8	832.8	** ↑
Fast activity	In beam breaks	39.0	175.8	* ↑
Slow activity	In beam breaks	232.9	657.0	*** ↑
Total static counts	In beam breaks	261.0	779.8	** ↑
Total mobile counts	In beam breaks	15.5	53.0	** ↑
Total rearing counts	In beam breaks	6.0	32.0	* ↑
Active time	In seconds	177.2	447.1	** ↑
Static time	In seconds	171.2	426.1	* ↑
Rearing time	In seconds	17.9	92.7	* ↑
Front to back counts	In beam breaks	3.4	10.4	* ↑
Inactive time	In seconds	3365.6	3152.9	* ↓
Distance travelled	in meters	6.5	23.3	* ↑

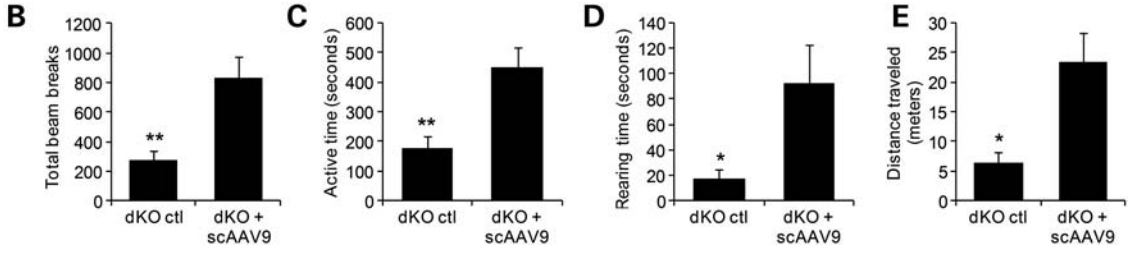

Figure 6. Improvement of physical activity and behaviour following scAAV9-U7ex23 injection. Mice were analysed at 10 weeks of age with open-field behavioural activity cages. (**A**) The 12 most relevant out of 22 recorded parameters are reported. Arrows indicate an increase (↑) or a decrease (↓) in the value of the measured parameter for the treated dKO mice compared with untreated controls. (**B**) Total activity, (**C**) total active time, (**D**) rearing time and (**E**) distance travelled are represented as graphs. $^{*}P < 0.05$, $^{**}P < 0.01$ and $^{***}P < 0.005$ compared with untreated dKO mice. Error bars are shown as mean ± SEM ($n = 6$ per cohort).

sacrifice them. Total RNA was extracted from blood serum from 40-week-old-treated dKO mice and qPCR was utilized to calculate the relative expression of miR-1 and miR-206 in untreated and treated mice to healthy controls. miR-223 expression was used as an endogenous control for $\Delta\Delta C_t$ analysis as described previously (29). As expected, dKO mice displayed much higher levels of miR-1 and miR-206 in the blood compared with wild-type controls (Fig. 8A and B). scAAV9-treated dKO mice on the other hand showed a remarkable reduction in the levels of miR-1 and miR-206, reflecting the benefit of the exon-skipping treatment.

We also demonstrated that treated dKO mice displayed a massive reduction in serum creatine kinase levels when compared with untreated dKO mice (Fig. 8C). This significant drop indicates a whole-body reduction in muscle degeneration consistent with the widespread restoration of dystrophin expression. Finally, we analysed circulating levels of aspartate aminotransferase (AST) and alanine aminotransferase (ALT), which are present in a variety of extrahepatic tissues, including cardiac and skeletal muscles. In both cases, levels were significantly lower in scAAV-treated dKO mice (Fig. 8D and E), indicating that restored dystrophin protein improved the integrity of muscle sarcolemma. Analysis of all the above biomarker levels confirms that the widespread restoration of dystrophin expression induced by the scAAV9-U7ex23-mediated exon skipping greatly improves muscle function in the long term in dKO mice.

DISCUSSION

In this study, we report the rescue of the severely affected dKO mouse model through AAV-mediated exon skipping. A single injection of scAAV9-U7ex23 leads to a considerable improvement of the dystrophic phenotype and muscle function of these mice accompanied by a remarkable extension of lifespan. Antisense-mediated exon skipping is one of the most promising approaches for the treatment of DMD, and early clinical trials have demonstrated encouraging results after both local and systemic administration of AOs. However, some substantial scientific barriers remain, especially regarding the personalized medicine nature of the strategy and the challenge of delivering to all affected tissues in DMD. The use of AAV vectors to deliver antisense sequences can circumvent some of these challenges as they offer the possibility of an efficient and stable transduction of all skeletal and cardiac muscles. While conventional AOs are still limited by a poor cellular uptake restricted to leaky muscle fibres, AAV vectors on the other hand transduce all muscle fibres equally efficiently regardless of their dystrophic/leaky state. The

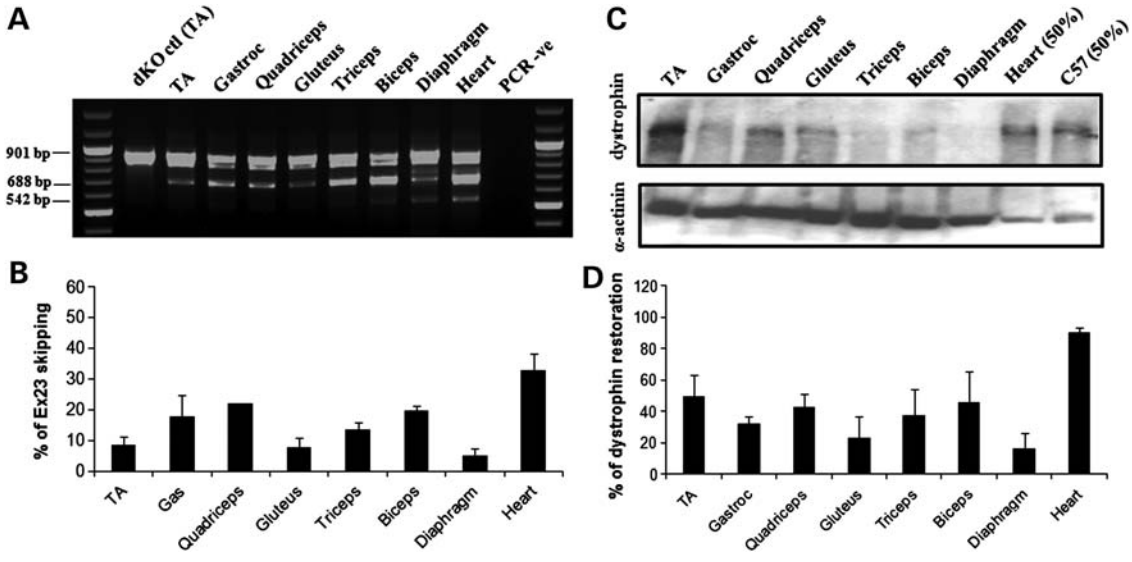

Figure 7. Analysis of exon-skipping and dystrophin expression at an endpoint in scAAV9-U7ex23-treated dKO mice. (**A**) RT–PCR analysis to detect exon 23 skipping efficiency at the RNA level. The 901 bp product represents the full-length transcript, and the products of 688 and 542 bp represent transcripts that exclude exon 23 and exons 22 and 23, respectively. (**B**) Quantification of exon 23 skipping measured by Taqman qPCR. Exon 23 skipping is expressed as a percentage of total dystrophin, measured by the exon 4–5 expression level, after normalization with an endogenous control. (**C**) Western blot to detect dystrophin expression in tissues from scAAV9-treated dKO mice, compared with untreated dKO and C57BL6 control mice (top gel). Equal loading of 100 μg protein is shown for each sample with α-actinin expression detected as a loading control, except for the heart and the C57BL6 control, where only 50% were loaded (bottom gel). (**D**) Quantification of levels of dystrophin protein restored in various muscles. Membranes were converted to numerical pictures by scanning, and band intensities were analysed using the ImageJ 1.33a software. Dystrophin levels are expressed as percentage compared with levels in wild-type tissue.

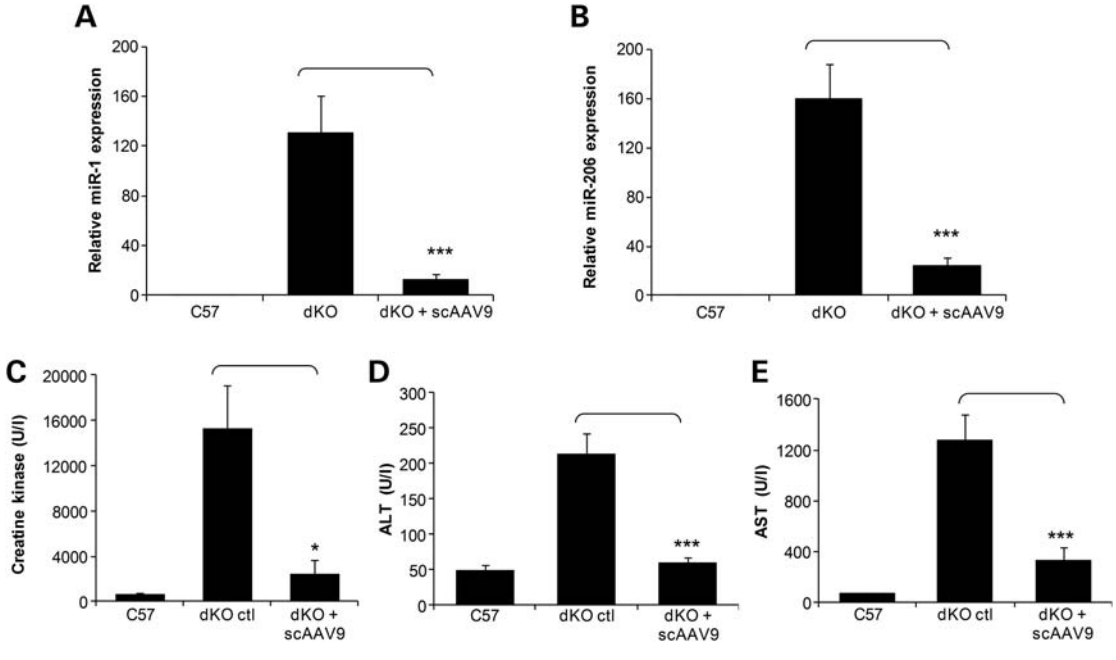

Figure 8. scAAV9-U7ex23 injection leads to a decrease in circulating biomarkers levels. (**A** and **B**) dKO mice were treated with a single i.v. injection of scAAV9-U7ex23 at 3 weeks of age, and blood serum was sampled at 40 weeks of age. Total RNA was extracted from serum and qPCR was utilized to calculate the relative expression of miR-1 and miR-206 in untreated and treated mice to healthy controls. miR-223 expression was used as an endogenous control for $\Delta\Delta C_t$ analysis as described previously (29). Data indicate the mean and standard deviation of the expression levels of a minimum of five mice for each treatment. $^{***}P < 0.001$. (**C**) Measurement of serum CK levels as an index of ongoing muscle membrane instability in scAAV9-U7ex23-treated dKO mice compared with untreated dKO mice ($^{*}P < 0.005$) and C57BL6 normal control mice. (**D** and **E**) Measurement of serum ALT and AST scAAV9-U7ex23-treated dKO mice compared with untreated dKO mice ($^{***}P < 0.001$) and C57BL6 normal control mice.

resulting dystrophin is more uniformly expressed within each muscle, as we observed in scAAV9-U7ex23-injected dKO mice. This could represent an advantage in clinical trials as the efficacy in humans will not be dependent on the number of leaky muscle fibres.

An additional challenge faced by AO-mediated exon skipping for DMD at present is the very little efficacy observed in the cardiac muscle (12,15). Clinically, cardiomyopathy is the second leading cause of death in patients with DMD in countries where ventilator therapy has been introduced, accounting for 10–40% of deaths in DMD populations (30), which implies a clear need for cardiac dystrophin correction. The reasons for the low efficiency of cardiac dystrophin restoration using AOs are unclear, but are probably related to the poor ability of unmodified oligonucleotides to penetrate the heart. In this study, on the other hand, we report particularly high levels of dystrophin expression in the heart following a single injection of scAAV9-U7ex23. This can be explained by the favourable tropism of the AAV serotype 9 for the cardiac muscle as described previously (17,18). The cardiac function was not assessed in dKO mice as we have previously reported that restoration of diaphragm and other respiratory muscle function was sufficient to prevent cardiomyopathy in dystrophic mice (31).

The causes of death in untreated dKO are still unclear and likely the result of respiratory failure and/or lack of food and water due to the severely decreased mobility towards the end of their life. The efficient restoration of dystrophin described here in the heart of treated dKO mice may have contributed to their extended lifespan. However, dKO mice can survive over 1 year even without cardiac dystrophin restoration as we demonstrated using peptide-conjugated AOs in earlier studies (31,32). It is therefore more plausible that the remarkable extension of dKO lifespan results from the widespread restoration of dystrophin throughout the whole body of dKO mice and especially the respiratory muscles.

Cell-penetrating peptide-conjugated AOs offer similar delivery advantages than AAV vectors as they have also addressed some of the issues faced by conventional AOs, such as efficient delivery to non-leaky fibres and the heart (33–37). They could therefore represent an effective strategy to reduce the dose level and dose frequency for clinical application. However, the toxicity of the current peptide chemistry poses a challenge for determination of an effective and safe regimen in man. One of these peptides, for example, was found to cause mild tubular degeneration in the kidneys of cynomolgus monkeys (37). The nature of the toxicity is not well understood, but it is likely to be due to the cationic nature of the peptide, impairing their clinical applicability at the current stage.

The main advantage of AAV vectors over naked or even conjugated AOs is the stability of the gene expression leading to a long-term restoration of dystrophin. In this work, we show that a single injection of scAAV9-U7ex23 is sufficient to rescue the severe dKO phenotype and remarkably extend lifespan. In order to evaluate the efficacy of the scAAV9-U7ex23 injection in the long term without sacrificing the injected mice, we investigated the levels of circulating biomarkers. In addition to the classic creatine kinase, AST and ALT levels, we analysed levels of miR-1 and miR-206, which have recently been reported to correlate with the severity of the pathology in DMD patients (29). All these biomarkers confirmed the long-term reduction in muscle degeneration consistent with the widespread restoration of dystrophin expression. These miRNAs released into the bloodstream represent ideal biomarkers to monitor the outcomes of therapeutic interventions, especially in older treated mice without the need to sacrifice them. Exon 23 skipping and dystrophin expression were still detected in treated animals 1 year after the injection, confirming the stability of AAV vectors in skeletal and cardiac muscles. Nonetheless, levels of skipping and protein were lower than those observed at 12 weeks of age, especially in the diaphragm, which may not have been sufficient to maintain the older dKO mice in healthy condition. Interestingly, this decrease in skipping and dystrophin levels correlated with the levels of U7ex23 transgene detected in the muscles (Supplementary Material, Fig. S3), indicating a loss of vector genome over time. This was somehow expected considering the severe and rapidly progressing pathology of dKO mice, imposing cycles of degeneration and regeneration to the muscles. Although the injection of scAAV9-U7ex23 induced widespread restoration of dystrophin, protecting the treated muscles, levels and distribution of dystrophin indicate that not all fibres were transduced or sufficiently rescued, allowing the pathological degeneration process to continue. Moreover, we must keep in mind that the exon-skipping strategy converts transduced dystrophic fibres into BMD-like fibres, which are known to be less resilient than normal ones as observed in very mild BMD patients.

We also noticed that the rescue of dKO mice required a minimal dose of 5E + 12 vg of scAAV9-U7ex23 injected, suggesting a threshold of dystrophin restoration necessary for the dKO survival. The few dKO mice injected with less than 5E + 12 vg displayed very low levels of dystrophin expression and only showed a very slight improvement of their phenotype and lifespan. While these observations might be concerning by suggesting the need of high doses of AAV vectors for translation, this may be explained by the early onset of dystrophy in these mice and the rapid and progressive nature of their pathology, which requires particularly high levels of dystrophin restoration. This requirement, which we had previously observed in our earlier study using peptide-conjugated AOs in dKO mice, suggests that the dKO model might not be appropriate for evaluating low-dose regimens (32). However, the comparatively longer time scale of disease progression in DMD patients might allow slow accumulation and restoration of dystrophin through low-dose treatment, which could be clinically applicable.

Although the use of AAV vectors offers many advantages such as long-term and widespread restoration of dystrophin as discussed above, they still face immunological challenges. Results from recent studies in larger animal models and in early human trials highlight immunological complications associated with viral vector-mediated gene transfer as the major barrier to clinical success. While AAV vectors do not elicit a cellular immune response in mice, multiple labs have now observed that AAVs 1, 2, 6 and 8 can elicit an immune response in the dog model for DMD (38–41), in monkeys (42) and in humans (43–47). However, studies in dystrophic dogs also showed that this T-cell response could be blocked

with transient immunosuppression (48), which has also been applied with success in non-human primates (42,49).

There is also some concern that dystrophin itself may be immunogenic in dystrophin-deficient patients. In the human trial of dystrophin gene transfer by Mendell *et al.* (50), intramuscular injections of rAAV2-minidystrophin resulted in robust mini-dystrophin-specific T-cell activity and none of the six patients injected displayed any detectable exogenous dystrophin. The authors proposed that dystrophin epitopes from revertant dystrophin fibres could prime the T-cell response. However, recent clinical trials evaluating AO-mediated exon skipping have not reported any immune response against the restored dystrophin (5–8), suggesting that restoration of dystrophin expression following intramuscular or systemic delivery will not necessarily trigger an immune response. Differing from a conventional gene therapy approach where the transgene expression is driven by a ubiquitous promoter, the AAV-U7snRNA system induces dystrophin expression only in cells naturally expressing it, which reduces the chances of activating the immune response through transduction of antigen-presenting cells. The AAV-U7snRNA approach may therefore circumvent this T-cell activation and represents the best of both worlds, combining the efficacy of a viral gene transfer system with the specificity of the exon-skipping strategy.

The use of viral vectors to shuttle antisense sequences also offers the possibility of delivering several U7snRNAs with the same vehicle, which could therefore target multiple exons. The number of DMD patients eligible for therapeutic exon skipping dramatically increases when considering double and multiexon skipping, reaching up to 83% of all DMD mutations. Of particular interest, the multiskipping of exons 45–55 in the hot-spot mutation region would be applicable to 63% of the patients and would also create a deletion associated with a mild phenotype (51). While double and multiexon skipping can be challenging using AOs (52), viral vectors can deliver different antisense constructs to the same nucleus, making the viral approach much more appealing to achieve multiexon skipping (53).

In conclusion, we report here a remarkable rescue of the dystrophic pathology in the severely affected dKO mice following a single injection of scAAV9-U7ex23. The improvement of the dKO phenotype and muscle function were not only demonstrated by electrophysiology on isolated muscle or observation of the mice (photos and videos), but also measured using open-field activity monitoring. This work represents an important milestone for the clinical application of the AAV-U7snRNA-mediated exon skipping approach, which is currently being planned for 2013.

MATERIALS AND METHODS

Viral vector production

For AAV vector production, the U7ex23 fragment was introduced between the ITR of a pscAAV construct for subsequent production of self-complementary vector. scAAV9-pseudotyped vectors were prepared by co-transfection in 293 cells of scAAV-U7ex23, pXX6 encoding adenovirus helper functions and pAAV9pITRCO2 that contains the AAV9 rep and cap genes. Vector particles were purified on Iodixanol gradients from cell lysates obtained 48 h after transfection and titres were measured by quantitative real-time PCR (54).

scAAV9-U7ex23 injections and animal experiments

dKO mice are generated by crossing (utr+/−, dys−/−) mice, which have been obtained by crossing the utr−/− mice (C57Bl6) with *mdx* mice (20). Approximately 1E + 13 vg of scAAV9-U7ex23 was delivered to dKO mice at 3 weeks of age, by i.v. injection in the tail vein with mice under general anaesthesia. Treated mice were killed at 13 weeks of age or at a humane endpoint by CO_2 inhalation. Muscles were snap-frozen in liquid nitrogen-cooled isopentane and stored at −80°C before further analysis. All animal experiments were carried out in Biomedical Science Building, University of Oxford, Oxford, UK, and performed according to the guidelines and protocols approved by the Home Office.

Open-field activity monitoring

The Linton AM1053 X, Y, Z IR Activity Monitors were used for open-field activity monitoring. Mice were acclimatized in empty cages for 90 min the day prior to actual data collection. The data were collected every 10 min over a 90 min period for 3 consecutive days. The first three of the nine recordings each day were disregarded upon analysis. Twenty-two different activity parameters were measured for each mouse, with total distance travelled, total activity, rearing time and total mobile counts considered the best parameters for monitoring behavioural activity.

Immunohistochemistry and histology

Sections of 8 μm were cut from at least two-thirds of the muscle length of the TA, gastrocnemius, quadriceps, glutaeus, biceps, triceps, diaphragm and cardiac muscle at 100 μm intervals. The intervening muscle sections were collected for subsequent RT–PCR analysis. Routine haematoxylin and eosin staining was used to examine the overall muscle morphology. The cryosections were then examined for dystrophin expression using the mouse monoclonal antibody NCL-DYS2 (Novocastra, UK). DAPC protein detection was also performed using mouse monoclonal antibodies to β-dystroglycan and α- and β-sarcoglycan according to the manufacturer's instructions (Novocastra). The polyclonal antibody was detected by goat-anti-rabbit IgGs Alexa 488 and the monoclonal antibodies were used with an M.O.M. kit (Vector Laboratories, Burlingame, CA, USA).

RNA isolation and RT–PCR analysis

Total RNA was isolated from intervening muscle sections collected during cryosection using TRIzol reagent according to the manufacturer's instructions (Invitrogen, UK). Aliquots of 200 ng of total RNA were used for RT–PCR analysis using the Access RT–PCR System (Promega) in a 50 μl reaction using the external primers Ex 20Fo (5′-CAGAATTCTG CCAATTGCTGAG-3′) and Ex 26Ro (5′-TTCTTCAGCTTGT GTCATCC-3′). The cDNA synthesis was carried out at 45°C

for 45 min, directly followed by the primary PCR of 30 cycles of 94°C (30 s), 58°C (1 min) and 72°C (2 min). Two microlitres of these reactions were then reamplified in nested PCRs by 22 cycles of 94°C (30 s), 58°C (1 min) and 72°C (2 min) using the internal primers Ex 20Fi (5′-CCCAGTCTACCACCC TATCAGAGC-3′) and Ex 26Ri (5′-CCTGCCTTTAAGGCTT CCTT-3′). PCR products were analysed on 2% agarose gels.

Quantitation of exon 23 skipping by quantitative PCR

RNA was isolated from mouse tissue as described above. Contaminating DNA was removed from the RNA preparations using the Turbo DNA-free system (Ambion). One-microgram aliquots of DNase-treated RNA were then subjected to reverse transcription using the First Strand synthesis system (Invitrogen) with random hexamers according to the manufacturer's instructions. qPCR was performed using Taqman assays that were designed against the exon 4–5 or exon 22–24 templates using the Custom Assay Design Tool (Applied Biosystems, primer/probe sequences available upon request). An inventoried 18S assay was utilized as an endogenous control (Applied Biosystems, 4310893E). Fifty nanograms of cDNA were used as an input per reaction and all assays were carried out in singleplex. Assays were performed under fast cycling conditions on an Applied Biosystems StepOne Plus thermocycler, and all data were analysed using the comparative C_t method using the associated StepOne analytical software. For a given sample, the delta-C_t values of exon 4–5 and exon 22–24 assays were used to calculate a relative abundance of total dystrophin and exon 23-skipped dystrophin mRNA, respectively. Exon 23 skipping was then expressed as a percentage against total dystrophin, as indicated by the exon 4–5 expression level.

Western blot analysis

Total protein was extracted from muscle samples with Newcastle buffer (3.8% sodium dodecyl sulphate, 75 mM Tris–HCl, pH 6.7, 4 M urea, 10% β-mercaptoethanol, 10% glycerol and 0.001% bromophenol blue) and quantified using the bicinchoninic acid protein assay kit, according to the manufacturer's instructions (Perbio Science, UK). Samples were denatured at 95°C for 5 min before 100 μg of protein was loaded in a 5% polyacrylamide gel with a 4% stacking gel. Gels were electrophoresed for 4–5 h at 100 V and blotted to a polyvinylidene difluoride membrane overnight at 50 V. Blots were blocked for 1 h with 10% non-fat milk in phosphate-buffered saline–Tween buffer. Dystrophin and α-actinin proteins were detected by probing the membrane with 1:100 dilution of NCL-DYS1 primary antibody (monoclonal antibody to dystrophin R8 repeat; Novocastra) and 1:200 dilution of α-actinin primary antibody (Santa Cruz Biotechnology), respectively. An incubation with a mouse horseradish peroxidase-conjugated secondary antibody (1:2000) or goat horseradish peroxidase-conjugated secondary antibody (1:160 000) allowed visualization using ECL Analysis System (GE Healthcare). Membranes were converted to numerical pictures by scanning, and band intensities were analysed using the ImageJ 1.33a software (http://rsb.info.nih.gov/ij/).

Muscle function analysis

Functional grip strength analysis was performed on treated and control mice at 12 weeks of age using a commercial grip strength monitor (Chatillon, UK). Each mouse was held 2 cm from the base of the tail, allowed to grip a bar attached to the apparatus with their fore paws and pulled gently until they released their grip. The force exerted was recorded from four sequential tests, averaged at 1 min apart. Specific force and force drop were measured from the EDL muscle dissected from the hind leg of the treated and control mice. During dissection and experiments, muscles were bathed in oxygenated (95% O_2–5% CO_2) Krebs–Hensley solution composing of (mM): NaCl, 118; $NaHCO_3$, 24.8, KCl, 4.75; KH_2PO_4, 1.18; $MgSO_4$, 1.18; $CaCl_2$, 2.54; and glucose, 10. Contractile properties were measured as described previously (32).

Biomarker level quantification from the serum

Blood samples were collected from tail bleeds under general anaesthesia. Analysis of serum creatine kinase (CK), ALT and AST levels was performed by the pathology laboratory (Mary Lyon Centre, Medical Research Council, Harwell, Oxfordshire, UK). Extraction and quantitation of miRNAs from serum: total RNA was extracted 25 μl aliquots of erythrocyte-free serum using Trizol LS (Invitrogen) according to the manufacturer's instructions, except that the RNA pellet was washed with 80% ethanol instead of 70%. Ten nanograms of total RNA of each sample to be analysed were then used as an input for reverse transcription using the microRNA Reverse Transcription Kit (Applied Biosystems) according to the manufacturer's instructions. Individual reverse transcription reactions were performed in the presence of a single miRNA-specific primer supplied with the corresponding TaqMan assay (Applied Biosystems), and each RNA sample was subjected to reverse transcription reactions for each of the miRNAs to be studied. Inventoried miRNA TaqMan qPCR assays were obtained from Applied Biosystems (Assay IDs: hsa-miR-1, hsa-miR-203, hsa-miR-223). qPCR was performed on the cDNA using an Applied Biosystems StepOne Plus thermocycler. All miRNA data were subjected to $\Delta\Delta C_t$ analysis using miR-223 expression levels as an endogenous control. For each of miR-1 and miR-206, expression levels in dKO and scAAV-treated mice were expressed relative to the mean expression of five healthy C57 control mice. Student's *t*-test analysis (two-tailed, unequal variance) was performed between the mean levels of relative miRNA expression of five untreated (dKO) and six treated (scAAV) mice.

Statistical analysis

All results are expressed as mean values ± SEM, unless otherwise stated. Differences between treated and control cohorts were determined using an unpaired Student's *t*-test.

SUPPLEMENTARY MATERIAL

Supplementary Material is available at *HMG* online.

ACKNOWLEDGEMENTS

We are grateful to Georges Dickson and Susan Jarmin for providing the scAAV construct. We would like to thank Dr Tertious Hough, Clinical Pathology Laboratory, Mary Lyon Centre, MRC, Harwell, UK, for clinical testing of blood samples.

Conflict of Interest statement. None declared.

FUNDING

This work was supported by the Medical Research Council (MRC), the Muscular Dystrophy Campaign (MDC), the Association Monegasque contre les myopathies (AMM), the Duchenne Parent Project de France (DPP France) and the Muscular Dystrophy Association of the USA (MDA).

REFERENCES

1. Monaco, A.P., Bertelson, C.J., Liechti-Gallati, S., Moser, H. and Kunkel, L.M. (1988) An explanation for the phenotypic differences between patients bearing partial deletions of the DMD locus. *Genomics*, **2**, 90–95.
2. Koenig, M., Beggs, A.H., Moyer, M., Scherpf, S., Heindrich, K., Bettecken, T., Meng, G., Muller, C.R., Lindlof, M., Kaariainen, H. *et al.* (1989) The molecular basis for Duchenne versus Becker muscular dystrophy: correlation of severity with type of deletion. *Am. J. Hum. Genet.*, **45**, 498–506.
3. Aartsma-Rus, A., Janson, A.A., Heemskerk, J.A., De Winter, C.L., Van Ommen, G.J. and Van Deutekom, J.C. (2006) Therapeutic modulation of DMD splicing by blocking exonic splicing enhancer sites with antisense oligonucleotides. *Ann. N. Y. Acad. Sci.*, **1082**, 74–76.
4. Mann, C.J., Honeyman, K., Cheng, A.J., Ly, T., Lloyd, F., Fletcher, S., Morgan, J.E., Partridge, T.A. and Wilton, S.D. (2001) Antisense-induced exon skipping and synthesis of dystrophin in the mdx mouse. *Proc. Natl Acad. Sci. USA*, **98**, 42–47.
5. van Deutekom, J.C., Janson, A.A., Ginjaar, I.B., Frankhuizen, W.S., Aartsma-Rus, A., Bremmer-Bout, M., den Dunnen, J.T., Koop, K., van der Kooi, A.J., Goemans, N.M. *et al.* (2007) Local dystrophin restoration with antisense oligonucleotide PRO051. *N. Engl. J. Med.*, **357**, 2677–2686.
6. Kinali, M., Arechavala-Gomeza, V., Feng, L., Cirak, S., Hunt, D., Adkin, C., Guglieri, M., Ashton, E., Abbs, S., Nihoyannopoulos, P. *et al.* (2009) Local restoration of dystrophin expression with the morpholino oligomer AVI-4658 in Duchenne muscular dystrophy: a single-blind, placebo-controlled, dose-escalation, proof-of-concept study. *Lancet Neurol.*, **8**, 918–928.
7. Goemans, N.M., Tulinius, M., van den Akker, J.T., Burm, B.E., Ekhart, P.F., Heuvelmans, N., Holling, T., Janson, A.A., Platenburg, G.J., Sipkens, J.A. *et al.* (2011) Systemic administration of PRO051 in Duchenne's muscular dystrophy. *N. Engl. J. Med.*, **364**, 1513–1522.
8. Cirak, S., Arechavala-Gomeza, V., Guglieri, M., Feng, L., Torelli, S., Anthony, K., Abbs, S., Garralda, M.E., Bourke, J., Wells, D.J. *et al.* (2011) Exon skipping and dystrophin restoration in patients with Duchenne muscular dystrophy after systemic phosphorodiamidate morpholino oligomer treatment: an open-label, phase 2, dose-escalation study. *Lancet*, **378**, 595–605.
9. Goyenvalle, A. and Davies, K.E. (2011) Challenges to oligonucleotides-based therapeutics for Duchenne muscular dystrophy. *Skelet. Muscle*, **1**, 8.
10. De Angelis, F.G., Sthandier, O., Berarducci, B., Toso, S., Galluzzi, G., Ricci, E., Cossu, G. and Bozzoni, I. (2002) Chimeric snRNA molecules carrying antisense sequences against the splice junctions of exon 51 of the dystrophin pre-mRNA induce exon skipping and restoration of a dystrophin synthesis in Delta 48–50 DMD cells. *Proc. Natl Acad. Sci. USA*, **99**, 9456–9461.
11. Goyenvalle, A., Vulin, A., Fougerousse, F., Leturcq, F., Kaplan, J.C., Garcia, L. and Danos, O. (2004) Rescue of dystrophic muscle through U7 snRNA-mediated exon skipping. *Science*, **306**, 1796–1799.
12. Alter, J., Lou, F., Rabinowitz, A., Yin, H., Rosenfeld, J., Wilton, S.D., Partridge, T.A. and Lu, Q.L. (2006) Systemic delivery of morpholino oligonucleotide restores dystrophin expression bodywide and improves dystrophic pathology. *Nat. Med.*, **12**, 175–177.
13. Heemskerk, H.A., de Winter, C.L., de Kimpe, S.J., van Kuik-Romeijn, P., Heuvelmans, N., Platenburg, G.J., van Ommen, G.J., van Deutekom, J.C. and Aartsma-Rus, A. (2009) *In vivo* comparison of 2′-*O*-methyl phosphorothioate and morpholino antisense oligonucleotides for Duchenne muscular dystrophy exon skipping. *J. Gene Med.*, **11**, 257–266.
14. Yokota, T., Lu, Q.L., Partridge, T., Kobayashi, M., Nakamura, A., Takeda, S. and Hoffman, E. (2009) Efficacy of systemic morpholino exon-skipping in Duchenne dystrophy dogs. *Ann. Neurol*, **65**, 667–676.
15. Lu, Q.L., Rabinowitz, A., Chen, Y.C., Yokota, T., Yin, H., Alter, J., Jadoon, A., Bou-Gharios, G. and Partridge, T. (2005) Systemic delivery of antisense oligoribonucleotide restores dystrophin expression in body-wide skeletal muscles. *Proc. Natl Acad. Sci. USA*, **102**, 198–203.
16. Trollet, C., Athanasopoulos, T., Popplewell, L., Malerba, A. and Dickson, G. (2009) Gene therapy for muscular dystrophy: current progress and future prospects. *Expert Opin. Biol. Ther.*, **9**, 849–866.
17. Zincarelli, C., Soltys, S., Rengo, G., Koch, W.J. and Rabinowitz, J.E. (2010) Comparative cardiac gene delivery of adeno-associated virus serotypes 1–9 reveals that AAV6 mediates the most efficient transduction in mouse heart. *Clin. Transl. Sci.*, **3**, 81–89.
18. Bish, L.T., Morine, K., Sleeper, M.M., Sanmiguel, J., Wu, D., Gao, G., Wilson, J.M. and Sweeney, H.L. (2008) Adeno-associated virus (AAV) serotype 9 provides global cardiac gene transfer superior to AAV1, AAV6, AAV7, and AAV8 in the mouse and rat. *Hum. Gene Ther.*, **19**, 1359–1368.
19. Grady, R.M., Teng, H., Nichol, M.C., Cunningham, J.C., Wilkinson, R.S. and Sanes, J.R. (1997) Skeletal and cardiac myopathies in mice lacking utrophin and dystrophin: a model for Duchenne muscular dystrophy. *Cell*, **90**, 729–738.
20. Deconinck, A.E., Rafael, J.A., Skinner, J.A., Brown, S.C., Potter, A.C., Metzinger, L., Watt, D.J., Dickson, J.G., Tinsley, J.M. and Davies, K.E. (1997) Utrophin-dystrophin-deficient mice as a model for Duchenne muscular dystrophy. *Cell*, **90**, 717–727.
21. McCarty, D.M., Monahan, P.E. and Samulski, R.J. (2001) Self-complementary recombinant adeno-associated virus (scAAV) vectors promote efficient transduction independently of DNA synthesis. *Gene Ther.*, **8**, 1248–1254.
22. Mann, C.J., Honeyman, K., McClorey, G., Fletcher, S. and Wilton, S.D. (2002) Improved antisense oligonucleotide induced exon skipping in the mdx mouse model of muscular dystrophy. *J. Gene Med.*, **4**, 644–654.
23. Spitali, P., Heemskerk, H., Vossen, R.H., Ferlini, A., den Dunnen, J.T., t Hoen, P.A. and Aartsma-Rus, A. (2010) Accurate quantification of dystrophin mRNA and exon skipping levels in Duchenne muscular dystrophy. *Lab. Invest.*, **90**, 1396–1402.
24. Brenman, J.E., Chao, D.S., Gee, S.H., McGee, A.W., Craven, S.E., Santillano, D.R., Wu, Z., Huang, F., Xia, H., Peters, M.F. *et al.* (1996) Interaction of nitric oxide synthase with the postsynaptic density protein PSD-95 and alpha1-syntrophin mediated by PDZ domains. *Cell*, **84**, 757–767.
25. Newey, S.E., Benson, M.A., Ponting, C.P., Davies, K.E. and Blake, D.J. (2000) Alternative splicing of dystrobrevin regulates the stoichiometry of syntrophin binding to the dystrophin protein complex. *Curr. Biol.*, **10**, 1295–1298.
26. Oliver, P.L., Keays, D.A. and Davies, K.E. (2007) Behavioural characterisation of the robotic mouse mutant. *Behav. Brain Res.*, **181**, 239–247.
27. Qiao, C., Li, J., Jiang, J., Zhu, X., Wang, B., Li, J. and Xiao, X. (2008) Myostatin propeptide gene delivery by adeno-associated virus serotype 8 vectors enhances muscle growth and ameliorates dystrophic phenotypes in mdx mice. *Hum. Gene Ther.*, **19**, 241–254.
28. Malerba, A., Sharp, P.S., Graham, I.R., Arechavala-Gomeza, V., Foster, K., Muntoni, F., Wells, D.J. and Dickson, G. (2011) Chronic systemic therapy with low-dose morpholino oligomers ameliorates the pathology and normalizes locomotor behavior in mdx mice. *Mol. Ther.*, **19**, 345–354.
29. Cacchiarelli, D., Legnini, I., Martone, J., Cazzella, V., D'Amico, A., Bertini, E. and Bozzoni, I. (2011) miRNAs as serum biomarkers for Duchenne muscular dystrophy. *EMBO Mol. Med.*, **3**, 258–265.

30. Muntoni, F., Torelli, S. and Ferlini, A. (2003) Dystrophin and mutations: one gene, several proteins, multiple phenotypes. *Lancet Neurol.*, **2**, 731–740.
31. Crisp, A., Yin, H., Goyenvalle, A., Betts, C., Moulton, H.M., Seow, Y., Babbs, A., Merritt, T., Saleh, A.F., Gait, M.J. *et al.* (2011) Diaphragm rescue alone prevents heart dysfunction in dystrophic mice. *Hum. Mol. Genet.*, **20**, 413–421.
32. Goyenvalle, A., Babbs, A., Powell, D., Kole, R., Fletcher, S., Wilton, S.D. and Davies, K.E. (2010) Prevention of dystrophic pathology in severely affected dystrophin/utrophin-deficient mice by morpholino-oligomer-mediated exon-skipping. *Mol. Ther.*, **18**, 198–205.
33. Yin, H., Moulton, H.M., Seow, Y., Boyd, C., Boutilier, J., Iverson, P. and Wood, M.J. (2008) Cell-penetrating peptide-conjugated antisense oligonucleotides restore systemic muscle and cardiac dystrophin expression and function. *Hum. Mol. Genet.*, **17**, 3909–3918.
34. Jearawiriyapaisarn, N., Moulton, H.M., Sazani, P., Kole, R. and Willis, M.S. (2010) Long-term improvement in mdx cardiomyopathy after therapy with peptide-conjugated morpholino oligomers. *Cardiovasc. Res.*, **85**, 444–453.
35. Wu, B., Moulton, H.M., Iversen, P.L., Jiang, J., Li, J., Li, J., Spurney, C.F., Sali, A., Guerron, A.D., Nagaraju, K. *et al.* (2008) Effective rescue of dystrophin improves cardiac function in dystrophin-deficient mice by a modified morpholino oligomer. *Proc. Natl Acad. Sci. USA*, **105**, 14814–14819.
36. Wu, B., Lu, P., Benrashid, E., Malik, S., Ashar, J., Doran, T.J. and Lu, Q.L. (2010) Dose-dependent restoration of dystrophin expression in cardiac muscle of dystrophic mice by systemically delivered morpholino. *Gene Ther.*, **17**, 132–140.
37. Moulton, H.M. and Moulton, J.D. (2010) Morpholinos and their peptide conjugates: therapeutic promise and challenge for Duchenne muscular dystrophy. *Biochim. Biophys. Acta*, **1798**, 2296–2303.
38. Wang, Z., Allen, J.M., Riddell, S.R., Gregorevic, P., Storb, R., Tapscott, S.J., Chamberlain, J.S. and Kuhr, C.S. (2007) Immunity to adeno-associated virus-mediated gene transfer in a random-bred canine model of Duchenne muscular dystrophy. *Hum. Gene Ther.*, **18**, 18–26.
39. Wang, Z., Storb, R., Lee, D., Kushmerick, M.J., Chu, B., Berger, C., Arnett, A., Allen, J., Chamberlain, J.S., Riddell, S.R. *et al.* (2010) Immune responses to AAV in canine muscle monitored by cellular assays and noninvasive imaging. *Mol. Ther.*, **18**, 617–624.
40. Yuasa, K., Yoshimura, M., Urasawa, N., Ohshima, S., Howell, J.M., Nakamura, A., Hijikata, T., Miyagoe-Suzuki, Y. and Takeda, S. (2007) Injection of a recombinant AAV serotype 2 into canine skeletal muscles evokes strong immune responses against transgene products. *Gene Ther.*, **14**, 1249–1260.
41. Yue, Y., Ghosh, A., Long, C., Bostick, B., Smith, B.F., Kornegay, J.N. and Duan, D. (2008) A single intravenous injection of adeno-associated virus serotype-9 leads to whole body skeletal muscle transduction in dogs. *Mol. Ther.*, **16**, 1944–1952.
42. Mingozzi, F., Hasbrouck, N.C., Basner-Tschakarjan, E., Edmonson, S.A., Hui, D.J., Sabatino, D.E., Zhou, S., Wright, J.F., Jiang, H., Pierce, G.F. *et al.* (2007) Modulation of tolerance to the transgene product in a nonhuman primate model of AAV-mediated gene transfer to liver. *Blood*, **110**, 2334–2341.
43. Mingozzi, F. and High, K.A. (2007) Immune responses to AAV in clinical trials. *Curr. Gene Ther.*, **7**, 316–324.
44. Mingozzi, F., Maus, M.V., Hui, D.J., Sabatino, D.E., Murphy, S.L., Rasko, J.E., Ragni, M.V., Manno, C.S., Sommer, J., Jiang, H. *et al.* (2007) CD8(+) T-cell responses to adeno-associated virus capsid in humans. *Nat. Med.*, **13**, 419–422.
45. Mendell, J.R., Rodino-Klapac, L.R., Rosales, X.Q., Coley, B.D., Galloway, G., Lewis, S., Malik, V., Shilling, C., Byrne, B.J., Conlon, T. *et al.* (2010) Sustained alpha-sarcoglycan gene expression after gene transfer in limb-girdle muscular dystrophy, type 2D. *Ann. Neurol.*, **68**, 629–638.
46. Mingozzi, F., Meulenberg, J.J., Hui, D.J., Basner-Tschakarjan, E., Hasbrouck, N.C., Edmonson, S.A., Hutnick, N.A., Betts, M.R., Kastelein, J.J., Stroes, E.S. *et al.* (2009) AAV-1-mediated gene transfer to skeletal muscle in humans results in dose-dependent activation of capsid-specific T cells. *Blood*, **114**, 2077–2086.
47. Manno, C.S., Pierce, G.F., Arruda, V.R., Glader, B., Ragni, M., Rasko, J.J., Ozelo, M.C., Hoots, K., Blatt, P., Konkle, B. *et al.* (2006) Successful transduction of liver in hemophilia by AAV-Factor IX and limitations imposed by the host immune response. *Nat. Med.*, **12**, 342–347.
48. Wang, Z., Kuhr, C.S., Allen, J.M., Blankinship, M., Gregorevic, P., Chamberlain, J.S., Tapscott, S.J. and Storb, R. (2007) Sustained AAV-mediated dystrophin expression in a canine model of Duchenne muscular dystrophy with a brief course of immunosuppression. *Mol. Ther.*, **15**, 1160–1166.
49. Jiang, H., Couto, L.B., Patarroyo-White, S., Liu, T., Nagy, D., Vargas, J.A., Zhou, S., Scallan, C.D., Sommer, J., Vijay, S. *et al.* (2006) Effects of transient immunosuppression on adenoassociated, virus-mediated, liver-directed gene transfer in rhesus macaques and implications for human gene therapy. *Blood*, **108**, 3321–3328.
50. Mendell, J.R., Campbell, K., Rodino-Klapac, L., Sahenk, Z., Shilling, C., Lewis, S., Bowles, D., Gray, S., Li, C., Galloway, G. *et al.* (2010) Dystrophin immunity in Duchenne's muscular dystrophy. *N. Engl. J. Med.*, **363**, 1429–1437.
51. Beroud, C., Tuffery-Giraud, S., Matsuo, M., Hamroun, D., Humbertclaude, V., Monnier, N., Moizard, M.P., Voelckel, M.A., Calemard, L.M., Boisseau, P. *et al.* (2007) Multiexon skipping leading to an artificial DMD protein lacking amino acids from exons 45 through 55 could rescue up to 63% of patients with Duchenne muscular dystrophy. *Hum. Mutat.*, **28**, 196–202.
52. van Vliet, L., de Winter, C.L., van Deutekom, J.C., van Ommen, G.J. and Aartsma-Rus, A. (2008) Assessment of the feasibility of exon 45-55 multiexon skipping for Duchenne muscular dystrophy. *BMC Med. Genet.*, **9**, 105.
53. Goyenvalle, A., Wright, J., Babbs, A., Wilkins, V., Garcia, L. and Davies, K.E. (2012) Engineering multiple U7snRNA constructs to induce single and multiexon-skipping for Duchenne muscular dystrophy. *Mol. Ther.*, 2012. doi:10.1038/mt.2012.26 [Epub ahead of print].
54. Goyenvalle, A., Babbs, A., van Ommen, G.J., Garcia, L. and Davies, K.E. (2009) Enhanced exon-skipping induced by U7 snRNA carrying a splicing silencer sequence: promising tool for DMD therapy. *Mol. Ther.*, **17**, 1234–1240.